Research Article

Cell cycle exit and neuronal differentiation 1-engineered embryonic neural stem cells enhance neuronal differentiation and neurobehavioral recovery after experimental traumatic brain injury

Ren Wang[1, #], Dian-Xu Yang[1, #], Ying-Liang Liu[2], Jun Ding[1], Yan Guo[1], Wan-Hai Ding[1, *], Heng-Li Tian[1, *], Fang Yuan[1, *]

Graphical Abstract *Cell cycle exit and neuronal differentiation 1-engineered embryonic neural stem cells promote neuronal differentiation and neurobehavioral recovery after experimental traumatic brain injury*
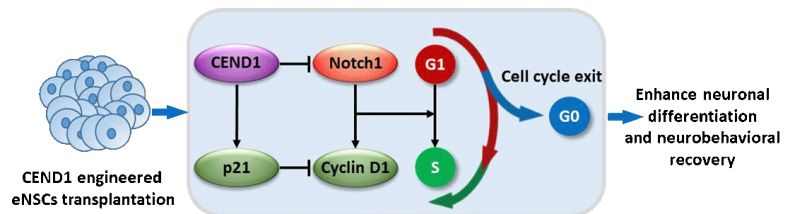
Abstract

Our previous study showed that cell cycle exit and neuronal differentiation 1 (CEND1) may participate in neural stem cell cycle exit and oriented differentiation. However, whether CEND1-transfected neural stem cells can improve the prognosis of traumatic brain injury remained unclear. In this study, we performed quantitative proteomic analysis and found that after traumatic brain injury, CEND1 expression was downregulated in mouse brain tissue. Three days after traumatic brain injury, we transplanted CEND1-transfected neural stem cells into the area surrounding the injury site. We found that at 5 weeks after traumatic brain injury, transplantation of CEND1-transfected neural stem cells markedly alleviated brain atrophy and greatly improved neurological function. *In vivo* and *in vitro* results indicate that CEND1 overexpression inhibited the proliferation of neural stem cells, but significantly promoted their neuronal differentiation. Additionally, CEND1 overexpression reduced protein levels of Notch1 and cyclin D1, but increased levels of p21 in CEND1-transfected neural stem cells. Treatment with CEND1-transfected neural stem cells was superior to similar treatment without CEND1 transfection. These findings suggest that transplantation of CEND1-transfected neural stem cells is a promising cell therapy for traumatic brain injury. This study was approved by the Animal Ethics Committee of the School of Biomedical Engineering of Shanghai Jiao Tong University, China (approval No. 2016034) on November 25, 2016.
Key Words: cell cycle exit and neuronal differentiation 1; cyclin D1; embryonic neural stem cells; neuronal differentiation; genetic engineering; overexpression; mice; Notch1; p21; traumatic brain injury

Chinese Library Classification No. R456; R741; Q789

Introduction

Traumatic brain injury (TBI) is caused by a sudden external assault to the head and often leads to brain damage, neurological disabilities, and/or death. Following TBI, efforts to promote neuronal regeneration are associated with improved functional outcomes (Bagnato and Boccagni, 2020; Willing et al., 2020). Thus, the transplantation of neural stem cells (NSCs) is a promising treatment for TBI-induced brain damage and neurological deficits (Chen et al., 2020; Jiang et al., 2020; Yasuhara et al., 2020). These transplanted cells secrete neurotrophins and can differentiate into functional neuronal cells to repair and replace damaged brain tissues (Xiong et

al., 2018). Furthermore, genetic engineering of stem cells has been identified as a promising strategy for improvement of neurogenesis to achieve better outcomes and avoid side effects (Li et al., 2018; Tang et al., 2018).

Cell cycle exit and neuronal differentiation 1 (CEND1), a neuronal lineage-specific regulator, is expressed at low levels in neuronal precursor cells and high levels in mature neurons (Koutmani et al., 2004). In subventricular zone-derived neurospheres, CEND1 overexpression promoted the exit of progenitor cells from the cell cycle, as well as their differentiation into neurons, via downregulation of cyclin D1 and inhibition of the Notch1/Hes1 pathway (Katsimpardi

[1]Department of Neurosurgery, Shanghai Jiao Tong University Affiliated Sixth People's Hospital, School of Medicine, Shanghai Jiao Tong University, Shanghai, China; [2]Department of Neurosurgery, Shanghai Tenth People's Hospital, Tongji University, Shanghai, China
*Correspondence to: Wan-Hai Ding, MD, PhD, dingwanhai@126.com; Heng-Li Tian, MD, PhD, tianhlsh@126.com; Fang Yuan, MD, PhD, yf021025@126.com.
https://orcid.org/0000-0001-7772-8233 (Ren Wang); https://orcid.org/0000-0002-4060-7830 (Fang Yuan)
#Both authors contributed equally to this work.

et al., 2008). Similarly, manipulation of CEND1 expression in neuroblastoma Neuro 2a cells reduced cyclin D1 levels through activation of the p53/pRb pathway, thereby leading to cell cycle arrest and neuronal conversion (Georgopoulou et al., 2006). Furthermore, CEND1 overexpression in Neuro 2a cells prevented adenosine triphosphate-induced proliferation and C2-ceramide-triggered apoptosis (Masgrau et al., 2009). Using proteomic analyses, we previously revealed a significant reduction in CEND1 expression levels at 24 hours after TBI (Ding et al., 2015). Because alterations in CEND1 expression are associated with the proliferation and neuronal differentiation of endogenous adult NSCs, CEND1-engineered embryonic NSCs (eNSCs) may enhance neuronal differentiation and improve outcomes after TBI (Makri et al., 2010).

Thus, the present study aimed to determine the efficacy of CEND1-engineered eNSC transplantation for the treatment of TBI in a mouse model of controlled cortical injury (CCI). The effects of treatment with CEND1-eNSCs on histological alleviation, functional recovery, cell proliferation, and neuronal differentiation were evaluated.

Materials and Methods

CCI mouse model
The mice were raised in an environment with a temperature of between 18–23°C and humidity of between 40–60% under 12-hour light/dark cycles. All experimental protocols involving animals were approved by the Animal Ethics Committee of the School of Biomedical Engineering of Shanghai Jiao Tong University, China (approval No. 2016034) on November 25, 2016. Adult male C57Bl/6 mice (aged 7–8 weeks, weighing 20–25 g) under specific pathogen-free conditions were provided by Shanghai SLAC Laboratory Animal Corp., Shanghai, China [License No. SCXK (Hu) 2017-0005]. Prior to induction of CCI, all mice were trained in the rotarod test for 3 consecutive days; animals that could not stand for at least 300 seconds were excluded from experiments. Mice were assessed in a model of TBI that employed CCI (PinPoint Precision Cortical Impactor PCI3000; Hatteras Instruments Inc., Cary, NC, USA), as previously described (Yuan et al., 2016). Briefly, mice were anesthetized and impacted with a 3-mm diameter impactor tip in accordance with the following injury severity parameters: velocity of 1.5 m/s, deformation depth of 1.5 mm, and dwell time of 85 ms.

Another 41 male adult C57Bl/6 mice underwent TBI surgery; of these 41 mice, four died in the first 3 days after surgery and three were excluded from analyses owing to a lack of obvious neurological deficits. Thus, 34 animals with similar post-surgery Garcia scores (Garcia et al., 1995) were randomly assigned into three treatment groups: phosphate-buffered saline (PBS) (n = 11), green fluorescent protein (GFP)-eNSCs (n = 11), and CEND1-eNSCs (n = 12). Next, the brain-injured mice were stereotactically injected with PBS, GFP-eNSCs, or CEND1-eNSCs. Garcia score, rotarod performance, and cognitive function of each group were evaluated during the 5-week period following the TBI procedure. Finally, mice were sacrificed for histological evaluations.

Quantitative proteomic analyses
Quantitative proteomic analyses were performed by Jingjie Bioscience Corp. (Hangzhou, China). Briefly, six mice were randomly divided into TBI and sham groups (n = 3 mice per group). Protein samples from the peri-contusion region were obtained 24 hours after surgery. Samples were grinded by liquid nitrogen and sonicated three times on ice. The protein was first precipitated with cold 15% trichloroacetic acid (Sigma, St. Louis, MO, USA) for 2 hours at –20°C, and then redissolved in buffer (8 M urea, 100 mM tetraethylammonium bromide, pH 8.0, Sigma). Protein concentration was determined with 2-D Quant kit (GE Healthcare, Pittsburgh, PA, USA) according to the

manufacturer's instructions. Approximately 100 µg protein for each sample digested with trypsin was used for the following experiments. After trypsin digestion, peptide was labeled with TMT (Thermo Fisher, Waltham, MA, USA) and fractionated by high-performance liquid chromatography. Finally, the resulting peptides were analyzed by high-resolution liquid chromatography-tandem mass spectrometry. Then, another six mice were randomly divided into TBI and sham groups (n = 3 mice per group), brain samples were obtained to validate the results of quantitative proteomic analyses by western blot.

Isolation, identification, proliferation, and differentiation of eNSCs
eNSCs were isolated from C57Bl/6 mouse embryos (Shanghai SLAC Laboratory Animal Corp., Shanghai, China) on embryonic day 14.5. To form neurospheres, frontal cortical tissues were digested into single-cell suspensions and subsequently cultured in T25 flasks with Dulbecco's Modified Eagle Medium with F-12 Nutrient Mixture (Gibco, Carlsbad, CA, USA) containing epidermal growth factor (20 ng/mL, Gibco), basic fibroblast growth factor (20 ng/mL, Gibco), L-glutamine (2 mM, Gibco), and B27 (2%, Gibco) supplement. To identify eNSCs, neurospheres were gently dissociated and planted on coverslips coated with poly-L-ornithine (20 µg/mL; Sigma) and laminin (20 µg/mL; Sigma). Next, cells were immunostained with goat anti-nestin (1:100; Cat# sc-21248; Santa Cruz Biotechnology, Dallas, TX, USA), mouse anti-TuJ1 (1:100; Cat# MAB1637; Millipore, Billerica, MA, USA), rabbit anti-glial fibrillary acidic protein (GFAP, Cat# AB5804, 1:100, Millipore), and rabbit anti-sex determining region Y-box 2 (SOX2; Cat# ab97959, 1:100; Abcam, Cambridge, UK) antibodies. To assess the proliferation of eNSCs, they were seeded in coated 96-well dishes at a density of 6×10^4 cells per well and assessed using Cell Counting Kit-8 (Dojindo, Kumamoto, Japan) for 6 days after transfection. To assess neuronal differentiation, eNSCs were cultured as a monolayer in differentiation medium comprised of Neurobasal medium (Gibco) containing B27 (2%) and L-glutamine (2 mM) supplement. After maintenance for 7 days, cells were immunostained with an anti-TuJ1 antibody (1:100, Millipore). All media were supplemented with antibiotics (1% penicillin and streptomycin, Gibco).

Transfection and transplantation of eNSCs
CEND1-GFP-PURO and control GFP-PURO lentiviruses were purchased from Hanbio Biotechnology Co., Ltd. (Shanghai, China), with a titer of 2×10^8 transducing units/mL. eNSCs were plated on dishes coated in laminin and poly-L-lysine in a proliferative culture solution. When cell cultures were 80% confluent, they were transfected with CEND1-GFP-PURO or control GFP-PURO lentiviruses; transfection efficiency was improved by the addition of puromycin (Sigma) to the culture medium.

Next, eNSCs were transplanted into the peri-injury regions at Target Point 1 (post bregma = –0.5 mm, lateral to the midline = 3 mm, depth = 1.5 mm), Target Point 2 (post bregma = –2 mm, lateral to the midline = 4.5 mm, depth = 1.5 mm), and Target Point 3 (post bregma = –3.5 mm, lateral to the midline = 3 mm, depth = 1.5 mm) at 3 days after TBI. Subsequently, an injection of PBS, eNSC control (eNSC transfected with control GFP-PURO lentiviruses), or CEND1-eNSCs (eNSC transfected with the CEND1-GFP-PURO lentiviruses) (3×10^5 cells in 3 µL PBS) was made into each target point at a rate of 1 µL/min using a Hamilton syringe and micro-infusion pump (WPI, Sarasota, FL, USA) attached to a stereotaxic device (Stoelting, Kiel, WI, USA).

Immunohistochemistry
Mice were anaesthetized with an overdose of 1% sodium pentobarbital (50 mg/kg; intraperitoneal injection; Sigma) and then perfused with 20 mL of ice-cold PBS (pH 7.4), followed by freshly hydrolyzed ice-cold 4% paraformaldehyde.

Research Article

Whole brain samples were harvested for subsequent immunohistochemistry. Free-floating brain sections (30-µm thick) were blocked with 10% normal goat serum and incubated overnight at 4°C with the following antibodies: goat anti-nestin, rabbit anti-GFAP, mouse anti-TuJ1, and rabbit anti-SOX2. Secondary fluorochrome-conjugated antibodies were donkey anti-mouse IgG-Alexa Fluor 594 (1:500; Cat# A21203; Invitrogen, Carlsbad, CA, USA), donkey anti-mouse IgG-Alexa Fluor 488 (1:500; Cat# A21202; Invitrogen), and donkey anti-rabbit IgG-Alexa Fluor 488 (1:500; Cat# A21206; Invitrogen), which were incubated for 1 hour at 37°C. Nuclear counterstaining was performed with 4′,6-diamidino-2-phenylindole dihydrochloride (DAPI, Sigma). Photographs were taken with a confocal microscope (Leica, Solms, Germany) for further analyses.

To identify and count GFP-positive (GFP$^+$) eNSCs, sections that crossed each transplantation target point were selected and three fields from the peri-injury region were randomly selected using either a 20× or 40× objective; care was taken to sample sections with similar anatomical features. Next, sections were incubated with the abovementioned primary antibodies and imaged (DM2500, Leica Microsystems, Wetzlar, Germany) under the same conditions by an investigator who was blinded to sample identification information. TuJ1$^+$/GFP$^+$ and GFAP$^+$/GFP$^+$ cells were counted and quantified for each image in the same blinded manner.

Western blot assay
Western blot analyses in the brain were carried out as previously described (Yuan et al., 2016). Primary antibodies included rabbit anti-CEND1(1:1000; Cat# ab113076; Abcam), mouse anti-tubulin (1:1000, Cat# ab7291; Abcam), rabbit anti-glyceraldehyde-3-phosphate dehydrogenase (GAPDH; 1:1000; Cat# 5174; Cell Signaling Technology, Beverly, MA, USA), rabbit anti-Notch1 (1:1000; Cat# 3608; Cell Signaling Technology), rabbit anti-cyclin D1 (1:1000; Cat# 2978; Cell Signaling Technology), and rabbit anti-p21 (1:1000; Cat# 2947; Cell Signaling Technology), which were incubated overnight at 4°C. After washing, membranes were incubated with an anti-rabbit horseradish peroxidase-conjugated secondary antibody (1:1000; Cat# 7074; Cell Signaling Technology) for 1 hour at room temperature and then reacted with an enhanced chemiluminescence substrate (Pierce, Rockford, IL, USA). Chemiluminescence was detected using Quantity One image software (Bio-Rad, Hercules, CA, USA), and relative intensities were calculated using Gel-Pro Analyzer software (Media Cybernetics, Bethesda, MD, USA).

Lesion volume and brain atrophy measurements
To determine lesion volume and the degree of brain atrophy, serial sections (30-µm thick) were collected from −0.5 mm to −3.5 mm posterior to bregma. The first of every ten consecutive sections was selected for staining with cresyl violet (Beyotime, Nantong, China). The areas of impact defects and remaining tissues were measured using ImageJ software (National Institutes of Health, Bethesda, MD, USA); lesion volume and atrophic volume were then calculated by multiplying the sum of all defects and the remaining areas by interval distance, respectively. Additionally, relative brain atrophy (%) was calculated using the following formula: (contralateral hemisphere volume − ipsilateral remaining volume)/contralateral hemisphere volume.

Neurobehavioral tests
An investigator who was blinded to the experimental groups performed the rotarod test, Morris Water maze (MWM) test, and neurological evaluations based on Garcia scoring. For the rotarod test, all mice were pre-trained for 3 days prior to CCI. After TBI had been induced, the average time (latency) to fall was recorded at 1, 2, 3, 4, and 5 weeks post-TBI (Yuan et al., 2016). Spatial memory was evaluated using the MWM

at 4 weeks post-TBI, as previously described (Liu et al., 2018). Briefly, during the training trials, mice were released into the pool from a randomly selected quadrant and given 60 seconds to locate the submerged platform; once the platform was found, each mouse was permitted to remain on the platform for 15 seconds. Each mouse performed four trials per day for 5 consecutive days. During the probe trial, the platform under the water was removed and the mice were allowed to swim freely for 60 seconds. The results are expressed as latency to find the platform and time spent in the target quadrant. Garcia scores were assessed at 1, 2, 3, 4, and 5 weeks post-TBI using a scale ranging from 0–18; this metric serves as a composite of scores for spontaneous activity, symmetry of movement (four limbs), symmetry of forelimbs, climbing, reaction to touch, and vibrissae touch (Yuan et al., 2016).

Statistical analysis
All values are presented as mean ± standard deviation (SD). All data analyses were performed using Student's *t*-test for two groups and one-way analysis of variance followed by Dunnett's *post hoc* test for three or more groups with GraphPad Prism version 6.02 software (GraphPad Software, Inc., La Jolla, CA, USA). Differences with $P < 0.05$ were considered statistically significant.

Results

CEND1 expression levels decrease after TBI
Quantitative proteomic analyses revealed altered expression levels of several proteins 24 hours after the induction of experimental TBI. Notably, there was a reduction in CEND1 levels in the brains of injured mice, implicating CEND1 in pathophysiological processes associated with TBI. Results of liquid chromatography with tandem mass spectrometry were validated by western blot analyses of CEND1 expression levels. Western blot results revealed a significant downregulation of CEND1 levels in peri-injured cerebral tissue regions compared with the sham group ($P < 0.01$; **Figure 1**).

CEND1 is successfully overexpressed in eNSCs
eNSCs were characterized by immunofluorescence staining, which revealed that the isolated cells were nestin$^+$ and SOX2$^+$, but TuJ1$^−$ and GFAP$^−$; these findings suggest that the cells were indeed eNSCs (**Figure 2A**). Lentivirus-based CEND1-GFP-PURO vector transduction was performed to manipulate CEND1 expression levels in eNSCs using a GFP-PURO lentivirus as a control. The CEND1-GFP-PURO virus was efficiently transfected into eNSCs, producing a GFP$^+$ rate of > 90% (**Figure 2B**). Furthermore, western blot results revealed a significant increase in CEND1 expression in CEND1-eNSCs compared with GFP-eNSCs ($P < 0.001$; **Figure 2C** and **D**). Thus, gene-engineered CEND1-eNSCs and GFP-eNSCs were used in subsequent experiments.

Transplantation of CEND1-engineered eNSCs reduces brain atrophy post-TBI
The experimental process is illustrated in **Figure 3A**. CEND1-engineered and control eNSCs were transplanted into mouse brains at 3 days after TBI; histological examinations and neurological function assessments were then carried out for up to 5 weeks after TBI. To evaluate the treatment effects of eNSC transplantation on damaged brains, consecutive brain sections were stained with cresyl violet at 5 weeks post-TBI (**Figure 3B**). CCI in mice resulted in significant defects in the brain parenchyma. The mean lesion volume of the PBS group was 9.54 ± 0.65 mm^3, but the contusion volume was significantly decreased in both GFP-eNSCs and CEND1-eNSCs groups compared with the PBS group (both $P < 0.01$; **Figure 3B** and **C**). Furthermore, there were significant reductions in brain atrophy volume in GFP-NSCs and CEND1-eNSCs groups compared with the PBS group ($P < 0.01$). Moreover, there was a smaller atrophic volume in the CEND1-eNSCs group

compared with the GFP-eNSCs group ($P < 0.01$; **Figure 3D**).

Transplantation of CEND1-engineered eNSCs improves neurobehavioral function after TBI

To explore the effects of CEND1-eNSCs treatment on post-TBI neurological outcomes, Garcia scores and performances on the rotarod test and MWM were assessed. Compared with the PBS group, CEND1-eNSCs and GFP-eNSCs groups exhibited significant improvements in Garcia scores at 3 weeks (both $P < 0.01$), 4 weeks ($P < 0.001$ and $P < 0.05$, respectively), and 5 weeks ($P < 0.001$ and $P < 0.05$, respectively) post-TBI. Additionally, Garcia scores were significantly improved in the CEND1-eNSCs group versus the GFP-eNSCs group at 4 and 5 weeks (both $P < 0.05$; **Figure 4A**). Rotarod test results also revealed significant improvements in motor function in the eNSCs treatment groups at 3 weeks (both $P < 0.001$), 4 weeks (both $P < 0.001$), and 5 weeks (both $P < 0.001$) post-TBI compared with the PBS group; moreover, the performance of the CEND1-eNSCs group was better than that of the GFP-eNSCs group at 3, 4, and 5 weeks ($P < 0.05$ or $P < 0.01$; **Figure 4B**). During training trials for the MWM, the latency to locate the hidden platform was shorter in mice that had undergone eNSCs transplantation compared with mice in the PBS group. Additionally, there was a significant decrease of time to find the platform at 32 and 33 days post-TBI in the CEND1-eNSCs group compared with the GFP-eNSCs group ($P < 0.05$; **Figure 4C**). During the probe trial, eNSCs-treated mice remained in the target quadrant for a significantly longer period compared with the PBS group ($P < 0.01$; **Figure 4D**); moreover, the CEND1-eNSCs group remained in the target quadrant for a significantly longer period compared with the GFP-eNSCs group (**Figure 4D** and **E**). Taken together, these findings suggest that transplantation of CEND1-overexpressing eNSCs improved memory deficits after TBI.

Transplantation of CEND1-engineered eNSCs promotes neuronal differentiation after TBI

To determine whether CEND1 mediated neuronal differentiation of transplanted eNSCs, grafted GFP$^+$ eNSCs (**Figure 5A**) were counterstained with lineage-specific phenotype markers. Compared with the GFP-eNSCs group, the CEND1-eNSCs group exhibited a significant increase in the percentage of TuJ1$^+$/GFP$^+$ neurons ($18.10 \pm 1.4\%$ vs. $27 \pm 1.2\%$, $P < 0.001$; **Figure 5B** and **D**) and a significant reduction in the percentage of GFAP$^+$/GFP$^+$ astrocytes ($75.68 \pm 0.8\%$ vs. $67.2 \pm 1.5\%$, $P < 0.001$) at 5 weeks post-TBI (**Figure 5C** and **E**), indicating that CEND1 overexpression promoted the neuronal differentiation of grafted eNSCs.

CEND1 inhibits eNSC proliferation and enhances eNSC differentiation *in vitro*

To determine whether CEND1 was involved in the regulation of eNSC proliferation, cells transfected with or without CEND1 were seeded on six-well dishes and allowed to adhere overnight; cell proliferation was subsequently quantified for up to 6 days using a Cell Counting Kit-8. Overexpression of CEND1 inhibited eNSC proliferation at 4 and 6 days after cell plating, as indicated by a significant reduction in the proliferation of CEND1 cells compared with cells transfected with the GFP control (**Figure 6A**). Furthermore, these reductions in the proliferative activity of eNSCs were associated with cell cycle exit and differentiation. Protein levels of cyclin D1, p21, and Notch1 were estimated in CEND1-transduced or GFP-control eNSCs using western blot analyses (**Figure 6B**). CEND1 overexpression markedly affected protein levels of cyclin D1, p21, and Notch1. Next, the neuronal differentiation of eNSCs was evaluated *in vitro* by immunostaining for TuJ1 (**Figure 6C**). Compared with the GFP-control group, the CEND1-eNSCs group exhibited significant increases in percentages of TuJ1$^+$GFP$^+$/GFP$^+$ cells ($25.6 \pm 3.7\%$ vs. $74.67 \pm 4.4\%$, $P < 0.001$) and TuJ1$^+$/total cells ($24.4 \pm 4.8\%$ vs. $66.7 \pm 3.5\%$, $P <$

0.001; **Figure 6D**). Thus, CEND1 overexpression significantly increased numbers of TuJ1$^+$/GFP$^+$ cells, indicating enhanced neuronal differentiation.

Discussion

The present study demonstrated that transplantation of eNSCs (with or without CEND1 overexpression) at 3 days after TBI significantly reduced lesion volume and improved neurological outcomes at 5 weeks after TBI. Additionally, CEND1 overexpression significantly improved the neuronal differentiation of transplanted eNSCs and CEND1-engineered eNSCs compared with independent treatment involving the grafting of GFP-eNSCs. Thus, these findings indicate that cell therapy using CEND1-engineered eNSCs was effective for the treatment of TBI.

To the best of our knowledge, this is the first study to show significantly decreased CEND1 expression levels at 24 hours post-TBI. Although CEND1 is highly expressed in differentiated neurons in the adult central nervous system (Weng et al., 2013), its expression levels are low in neuroepithelial precursors and radial glia in the developing central nervous system, when these cells are destined to differentiate into the neuronal lineage . Importantly, CEND1 is not expressed in progenitor cells prior to their development into neuroglial cells (Koutmani et al., 2004). More recent studies have demonstrated that CEND1 reduces the proliferation of neuroblastoma cells and induces neuronal differentiation (Georgopoulou et al., 2006); additionally, CEND1 overexpression in the developing central nervous system of chickens can induce neural precursors to exit the cell cycle and differentiate into neuronal cells (Politis et al., 2007). Similarly, manipulation of CEND1 expression has been shown to promote the transition of postnatal mammalian brain-derived neurospheres into mature neurons (Katsimpardi et al., 2008). Taken together, these results suggest that alterations in CEND1 expression may be involved in pathophysiological processes that influence the proliferation and differentiation of endogenous NSCs to promote functional recovery after TBI.

To verify this hypothesis, lentiviruses were used to overexpress CEND1, and the consequences of this overexpression on proliferation and differentiation of eNSCs were examined. CEND1 overexpression significantly reduced eNSC proliferation, but facilitated the neuronal differentiation of eNSCs. The number of eNSCs was relatively lower in the CEND1 group compared with the eNSCs control group at 4 and 6 days after cell plating, indicating that CEND1 overexpression was sufficient for the reduction of eNSC proliferative activity. Furthermore, results of an *in vitro* differentiation assay revealed that TuJ1 expression increased when eNSCs were CEND1-engineered to promote differentiation towards a neuronal lineage. To evaluate the effects of CEND1 on differentiation of eNSCs *in vivo*, genetically engineered eNSCs were transplanted into the brains of mice at 3 days after TBI. Consistent with the results of previous *in vitro* studies, CEND1 overexpression significantly increased numbers of TuJ1$^+$/GFP$^+$ neurons, but reduced numbers of GFAP$^+$/GFP$^+$ astrocytes. These results indicate that CEND1 was sufficient to arrest proliferation of eNSCs, but could enhance their differentiation toward neurons.

The first step in NSC differentiation is exiting the cell cycle; thus, cell cycle regulation plays an important role in neural cell proliferation and differentiation (Liu et al., 2019). An increased G1 duration is strongly correlated with cell cycle exit, as well as the neuronal differentiation of progenitor cells (Lukaszewicz et al., 2002); CEND1 is known to lengthen the G1/S transition of NSCs by downregulating cyclin D1 levels, thereby leading to enhanced neuronal differentiation (Dehay and Kennedy, 2007). The present study also examined cell cycle regulator changes in CEND1-overexpressing eNSCs
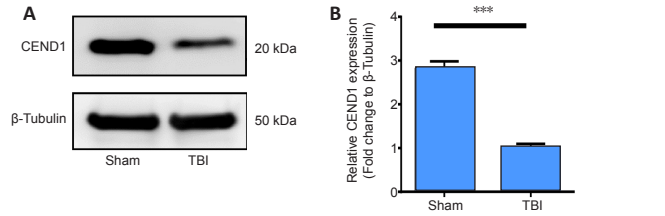
Figure 1 | TBI reduces CEND1 expression levels in cerebral tissues.
(A) Western blot analyses verified changes in CEND1 expression levels. (B) Protein expression levels were normalized to β-tubulin for quantitative analysis. Data are presented as mean ± SD (n = 3) from three independent experiments. ***P < 0.001 (Student's t-test). CEND1: Cell cycle exit and neuronal differentiation 1; TBI: traumatic brain injury.
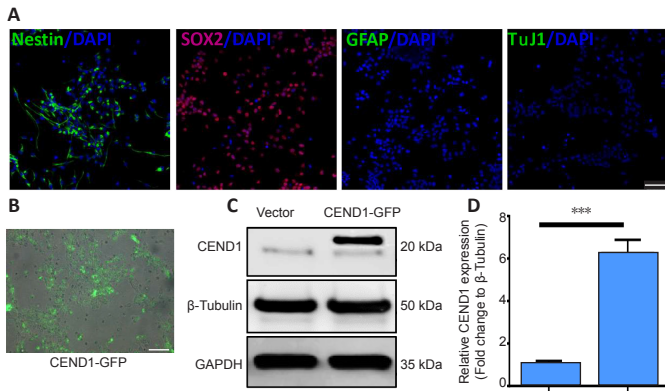

Figure 2 | Successful transfection of a CEND1-overexpressing lentivirus into eNSCs *in vitro*.
(A) eNSCs were characterized by immunofluorescence staining with nestin (green, stained by Alexa Fluor 488), SOX2 (red, stained by Alexa Fluor 594), GFAP (green, stained by Alexa Fluor 488), and TuJ1 (green, stained by Alexa Fluor 488). (B) CEND1-GFP-transfected eNSCs in bright field and fluorescent field were merged to assess transfection efficacy. Scale bars: 50 μm in A, 200 μm in B. (C, D) Western blot analyses validated elevated CEND1 protein expression levels in GFP-eNSCs (vector) and CEND1-GFP-eNSCs. Data are presented as mean ± SD (n = 3) from three independent experiments. ***P < 0.001 (Student's t-test). CEND1: Cell cycle exit and neuronal differentiation 1; DAPI: 4′,6-diamidino-2-phenylindole dihydrochloride; eNSC: embryonic neural stem cell; GAPDH: glyceraldehyde-3-phosphate dehydrogenase; GFAP: glial fibrillary acidic protein; GFP: green fluorescent protein; SOX2: sex determining region Y-box 2; TuJ1: neuronal class III β-tubulin.
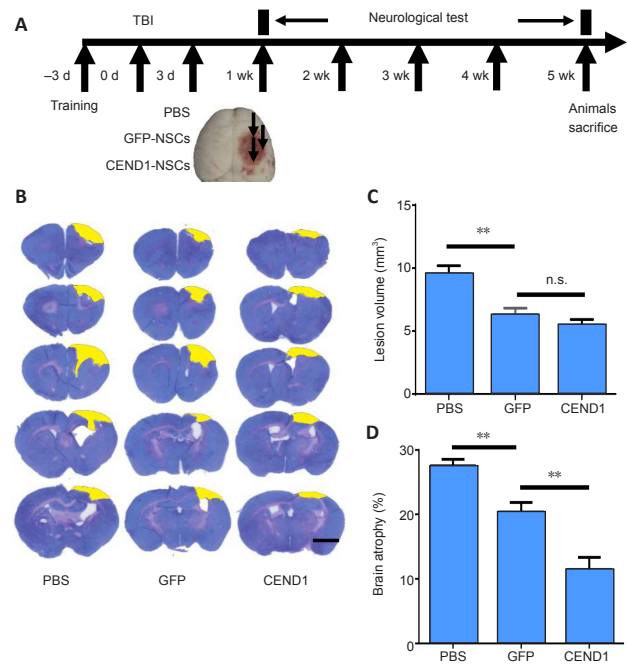

Figure 3 | Transplantation of CEND1-engineered eNSCs protects against TBI-induced brain atrophy.
(A) Timeline of experiments. Behavioral training was performed 3 days prior to TBI and eNSCs were transplanted into mouse brains at 3 days after TBI; outcomes were measured at the indicated intervals. Arrows indicate the targeted points. (B) Representative cresyl violet-stained brain sections from PBS, GFP-eNSCs, and CEND1-eNSCs groups at 5 weeks after TBI. Lesion volume was significantly reduced in GFP-eNSCs and CEND1-eNSCs groups compared with the PBS group. Lesions are outlined in yellow. Scale bar: 1 mm. (C) Transplantation of GFP-eNSCs and CEND1-eNSCs significantly reduced cortical contusion volumes. (D) Brain atrophy was alleviated in GFP-eNSCs and CEND1-eNSCs groups compared with the PBS group; CEND1-eNSCs treatment further reduced brain atrophy compared with the GFP-eNSCs group. Data are presented as mean ± SD (n = 11 in PBS and GFP-eNSCs groups, n = 12 in the CEND1-eNSCs group) from three independent experiments. **P < 0.01 (one-way analysis of variance followed by Dunnett's test). CEND1: Cell cycle exit and neuronal differentiation 1; eNSC: embryonic neural stem cell; GFP, green fluorescent protein; n.s.: not significant; PBS: phosphate-buffered saline; TBI: traumatic brain injury.
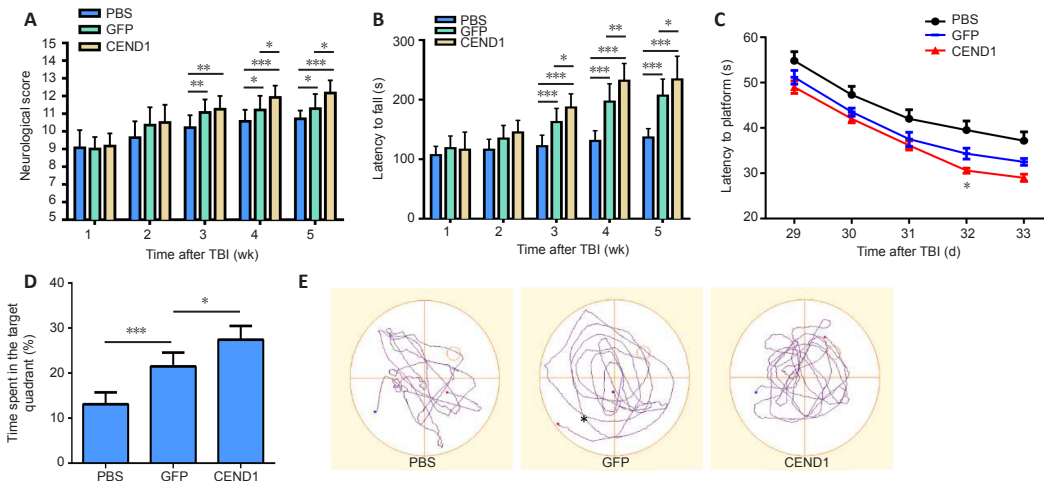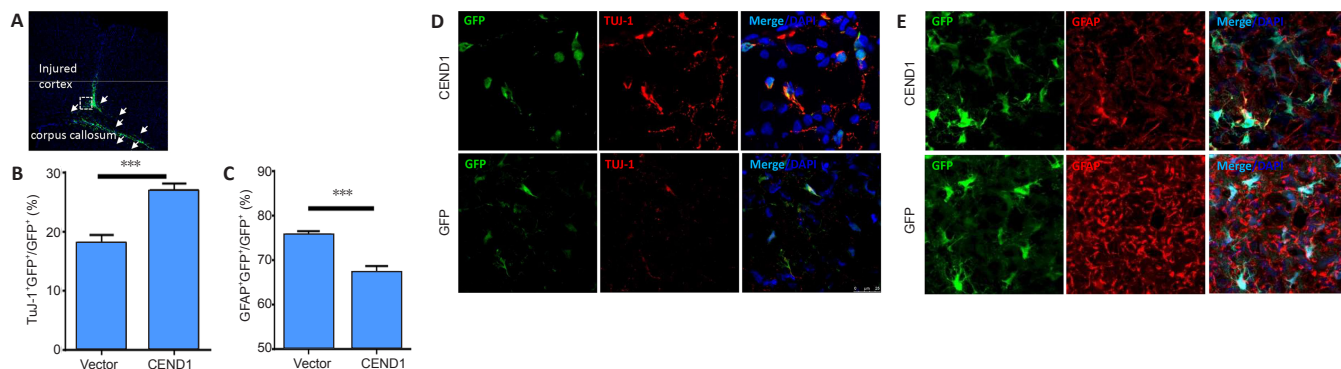

Figure 4 | Transplantation of CEND1-overexpressing eNSCs improves neurobehavioral recovery after TBI.
Neurological scores (Garcia score), performances on the rotarod test, and MWM were evaluated within 5 weeks after TBI. (A) After TBI, the GFP-eNSCs group had significantly higher scores at the indicated times compared with the PBS group; the CEND1-eNSCs group exhibited further improvements. (B) The results of the rotarod test revealed similar improvement trends in GFP-eNSCs and CEND1-eNSCs groups. (C) In training sessions for the MWM, latencies to find the hidden platforms were shorter in the eNSC-treated groups than in the PBS-treated group; the CEND1-eNSCs group required less time to find the platform on Days 32 and 33 post-TBI, compared with the GFP-eNSCs group. (D, E) Percent of time spent (D) and representative swimming traces (E) in the target quadrant during the probe trial session at 5 weeks after TBI. Time spent in the target quadrant was longer in GFP-eNSCs and CEND1-eNSCs groups compared with the PBS group. CEND1-eNSCs treatment further increased time spent in the target quadrant compared with the GFP-eNSCs group. Data are presented as mean ± SD (n = 11–12 mice/group) from three independent experiments. *P < 0.05, **P < 0.01, ***P < 0.001 (one-way analysis of variance followed by Dunnett's test). CEND1: Cell cycle exit and neuronal differentiation 1; eNSC: embryonic neural stem cell; GFP: green fluorescent protein; n.s.: not significant; PBS: phosphate-buffered saline; TBI: traumatic brain injury.

Figure 5 | Transplantation of CEND1-eNSCs promotes neuronal differentiation in the injured mouse brain.
(A) Representative image of GFP$^+$ cells from GFP-eNSCs therapy mouse brain 5 weeks after TBI. Dotted box indicates area for imaging and statistical analysis. Arrows indicate transplanted eNSCs. (B, D) Quantification of TuJ1$^+$/GFP$^+$ cells and double immunostaining of TuJ1$^+$ (red, stained by Alexa Fluor 594) and GFP$^+$ cells in peri-injured cerebral regions at 5 weeks post-TBI. Compared with the GFP-control group, the CEND1-eNSCs group exhibited a significant increase in the percentage of TuJ1$^+$/GFP$^+$ neurons. (C, E) Quantification of GFAP$^+$GFP$^+$/GFP$^+$ cells and double immunostaining of GFAP$^+$ (red, stained by Alexa Fluor 594) and GFP$^+$ cells in peri-injured cerebral regions at 5 weeks post-TBI. Compared with the GFP-control group, the CEND1-eNSCs group exhibited a significant reduction in the percentage of GFAP$^+$/GFP$^+$ astrocytes. Scale bar: 50 μm. Data are presented as mean ± SD ($n = 6$) from three independent experiments. ***$P < 0.001$ (one-way analysis of variance followed by Dunnett's test). CEND1: Cell cycle exit and neuronal differentiation 1; eNSC: embryonic neural stem cell; GFAP: glial fibrillary acidic protein; GFP: green fluorescent protein; PBS: phosphate-buffered saline; TBI: traumatic brain injury; TuJ1: neuron-specific class III β-tubulin.
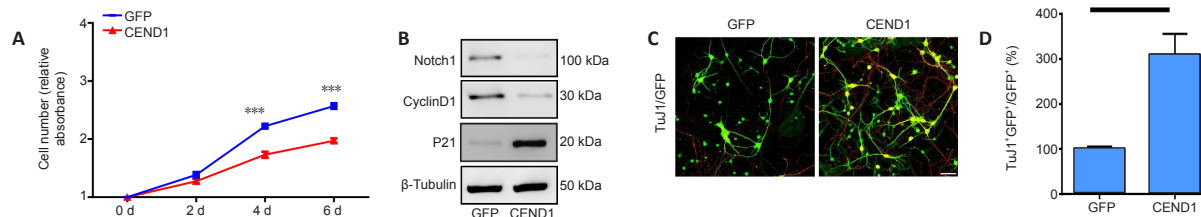

Figure 6 | CEND1 modulates the proliferation and differentiation of eNSCs *in vitro*.
(A) Cell Counting Kit-8 assays of cell proliferation. Overexpression of CEND1 significantly reduced eNSC proliferation. (B) Western blot analyses revealed significant reductions in Notch1 and cyclin D1 levels, as well as a significant increase in p21 protein expression levels, in CEND1-eNSCs compared with GFP controls. (C) eNSCs transfected with or without CEND1 were immunostained with antibodies against TuJ1 (red, stained by Alexa Fluor 594). CEND1 overexpression significantly increased the percentage of TuJ1$^+$/GFP$^+$ cells. Scale bar: 50 μm. (D) Quantification of TuJ1$^+$GFP$^+$/GFP$^+$ cells (yellow, indicating merge of red and green) in the CEND1-overexpressing group, normalized to the GFP-control group. Data are presented as mean ± SD ($n = 3$) from three independent experiments. ***$P < 0.001$, *vs.* GFP group (Student's *t*-test). CEND1: Cell cycle exit and neuronal differentiation 1; eNSC: embryonic neural stem cell; GFP: green fluorescent protein; TuJ1: neuron-specific class III β-tubulin.

and found that CEND1 significantly reduced cyclin D1 levels while markedly increasing p21 levels. Knockout of cyclin D1 in NSCs can induce G0/G1 cell cycle arrest and inhibit the differentiation of NSCs to astrocytes without impairing neuronal cell differentiation (Sumrejkanchanakij et al., 2003). Additionally, protein levels of p21 gradually increase during neuronal differentiation (Adepoju et al., 2014), whereas upregulation of p21 inhibits the proliferation of NSCs (Li and Wong, 2018). The present results, which showed that CEND1-induced coupling of neuronal differentiation with cell cycle exit is a result of cell cycle regulator modifications, are consistent with those of previous studies. The cellular mechanisms that underlie CEND1-mediated neuronal differentiation of NSCs also involve the activation of proneural genes and downregulation of the Notch1 pathway (Politis et al., 2007). Additionally, CEND1 overexpression in neonatal subventricular zone neural progenitors reduces protein levels of Notch1 and Hes1 (Politis et al., 2007). Similarly, the present study found that altered CEND1 expression caused significant downregulation of Notch1 levels. Taken together, these results suggest that CEND1 promoted the cell cycle withdrawal of NSCs and initiated neuronal differentiation, at least in part, by downregulating levels of cyclin D1 and Notch1, and upregulating the level of p21.

Many studies have demonstrated that NSC transplantation is an effective treatment following brain injury (Weston and Sun, 2018; Xiong et al., 2018; Yasuhara et al., 2020). However, this type of therapy has limited efficacy because NSCs typically differentiate into glial cells, rather than neurons (Weston and Sun, 2018). Stem cell treatments for TBI aim to generate cortical neuronal cells to repair the damaged brain; thus, efforts to promote the differentiation of NSCs into mature neurons and reduce astrocytosis may further restore brain tissue continuity and function. The present findings show that CEND1 overexpression enhanced the maturation of transplanted eNSCs into neurons and more effectively facilitated the repair of histological architecture in the brain compared with traditional eNSCs therapies. These results are consistent with the findings of a previous study that used a stab-induced cortical injury mouse model to show that treatment with CEND1-overexpressing eNSCs could promote tissue regeneration by increasing the number of mature neurons and reducing astroglial scarring (Makri et al., 2010). CEND1 can promote brain-derived neurotrophic factor (BDNF), as well as reelin secretion, to stimulate granule cell migration and Purkinje neuron differentiation during cerebellar development (Sergaki et al., 2010). However, the mechanism by which CEND1 regulates BDNF remains to be studied. The present findings suggest that regulation of BDNF expression and protein stabilization by CEND1 is linked with intracellular calcium signaling (Masgrau et al., 2009; Sergaki et al., 2010). The combined effect on neuronal differentiation and neurotrophic factor secretion may contribute to reducing the injured lesion volume after TBI. The present study also demonstrated that CEND1-engineered eNSCs more effectively improved long-term neurological function in brain-injured mice compared with independent grafting of NSCs, suggesting that CEND1 represents a potential target for TBI cell therapies. There are several limitations and biases of our study. First, we did not detect in depth what type of neurons eNSCs differentiated into following transplantation. Second,

mechanisms underlying how these neurons incorporate the remaining host neurons to fix damaged tissue and relieve neurobehavioral defects after TBI need further investigation. Finally, we did not evaluate the effects of CEND1 overexpression on oligodendrocyte lineage progression. Taken together, the present findings show that CEND1-engineered eNSCs were associated with better histological and neurological functional outcomes in mice with cortical injuries, even when grafted 3 days after TBI. These beneficial effects can be attributed to the inhibition of eNSC proliferation, reduction of astrocytosis, and promotion of neuronal differentiation during the 5 weeks after treatment. Thus, the present results suggest that CEND1-induced manipulation of eNSCs represents a promising cell therapy for the treatment of TBI.

References

Adepoju A, Micali N, Ogawa K, Hoeppner DJ, McKay RD (2014) FGF2 and insulin signaling converge to regulate cyclin D expression in multipotent neural stem cells. Stem Cells 32:770-778.

Bagnato S, Boccagni C (2020) Moderate/severe traumatic brain injury as a trigger of chronic neurodegeneration in humans. Neural Regen Res 15:1247-1248.

Chen JL, Shi XY, Cheng J, Ye YC, Zhang ZW, Li XH, Sun HT (2020) Protective effect of human umbilical cord blood mesenchymal stem cells on the rat's blood-brain barrier after traumatic brain injury. Zhongguo Zuzhi Gongcheng Yanjiu 24:3947-3952.

Dehay C, Kennedy H (2007) Cell-cycle control and cortical development. Nat Rev Neurosci 8:438-450.

Ding J, Ding Z, Yuan F, Guo J, Chen H, Gao W, Wang R, Gu Y, Chen J, Guo Y, Tian H (2015) Proteomics analysis after traumatic brain injury in rats: the search for potential biomarkers. Arq Neuropsiquiatr 73:342-349.

Gaitanou M, Segklia K, Matsas R (2019) Cend1, a story with many tales: from regulation of cell cycle progression/exit of neural stem cells to brain structure and function. Stem Cells Int 2019:2054783.

Garcia JH, Wagner S, Liu KF, Hu XJ (1995) Neurological deficit and extent of neuronal necrosis attributable to middle cerebral artery occlusion in rats. Statistical validation. Stroke 26:627-635.

Georgopoulou N, Hurel C, Politis PK, Gaitanou M, Matsas R, Thomaidou D (2006) BM88 is a dual function molecule inducing cell cycle exit and neuronal differentiation of neuroblastoma cells via cyclin D1 down-regulation and retinoblastoma protein hypophosphorylation. J Biol Chem 281:33606-33620.

Jiang JP, Liu XY, Zhao F, Zhu X, Li XY, Niu XG, Yao ZT, Dai C, Xu HY, Ma K, Chen XY, Zhang S (2020) Three-dimensional bioprinting collagen/silk fibroin scaffold combined with neural stem cells promotes nerve regeneration after spinal cord injury. Neural Regen Res 15:959-968.

Katsimpardi L, Gaitanou M, Malnou CE, Lledo PM, Charneau P, Matsas R, Thomaidou D (2008) BM88/Cend1 expression levels are critical for proliferation and differentiation of subventricular zone-derived neural precursor cells. Stem Cells 26:1796-1807.

Koutmani Y, Hurel C, Patsavoudi E, Hack M, Gotz M, Thomaidou D, Matsas R (2004) BM88 is an early marker of proliferating precursor cells that will differentiate into the neuronal lineage. Eur J Neurosci 20:2509-2523.

Li Y, Chang S, Li W, Tang G, Ma Y, Liu Y, Yuan F, Zhang Z, Yang GY, Wang Y (2018) cxcl12-engineered endothelial progenitor cells enhance neurogenesis and angiogenesis after ischemic brain injury in mice. Stem Cell Res Ther 9:139.

Li YQ, Wong CS (2018) Effects of p21 on adult hippocampal neuronal development after irradiation. Cell Death Discov 4:15.

Liu L, Michowski W, Kolodziejczyk A, Sicinski P (2019) The cell cycle in stem cell proliferation, pluripotency and differentiation. Nat Cell Biol 21:1060-1067.

Liu YL, Yuan F, Yang DX, Xu ZM, Jing Y, Yang GY, Geng Z, Xia WL, Tian HL (2018) Adjudin attenuates cerebral edema and improves neurological function in mice with experimental traumatic brain injury. J Neurotrauma 35:2850-2860.

Lukaszewicz A, Savatier P, Cortay V, Kennedy H, Dehay C (2002) Contrasting effects of basic fibroblast growth factor and neurotrophin 3 on cell cycle kinetics of mouse cortical stem cells. J Neurosci 22:6610-6622.

Makri G, Lavdas AA, Katsimpardi L, Charneau P, Thomaidou D, Matsas R (2010) Transplantation of embryonic neural stem/precursor cells overexpressing BM88/Cend1 enhances the generation of neuronal cells in the injured mouse cortex. Stem Cells 28:127-139.

Masgrau R, Hurel C, Papastefanaki F, Georgopoulou N, Thomaidou D, Matsas R (2009) BM88/Cend1 regulates stimuli-induced intracellular calcium mobilization. Neuropharmacology 56:598-609.

Politis PK, Makri G, Thomaidou D, Geissen M, Rohrer H, Matsas R (2007) BM88/CEND1 coordinates cell cycle exit and differentiation of neuronal precursors. Proc Natl Acad Sci U S A 104:17861-17866.

Sergaki MC, Guillemot F, Matsas R (2010) Impaired cerebellar development and deficits in motor coordination in mice lacking the neuronal protein BM88/Cend1. Mol Cell Neurosci 44:15-29.

Sumrejkanchanakij P, Tamamori-Adachi M, Matsunaga Y, Eto K, Ikeda MA (2003) Role of cyclin D1 cytoplasmic sequestration in the survival of postmitotic neurons. Oncogene 22:8723-8730.

Tang H, Li Y, Zhang J (2018) Brain injury and stem cell replacement. Stem Cells Int 2018:5173494.

Weng L, Lin YF, Li AL, Wang CE, Yan S, Sun M, Gaertig MA, Mitha N, Kosaka J, Wakabayashi T, Xu X, Tang B, Li S, Li XJ (2013) Loss of Ahi1 affects early development by impairing BM88/Cend1-mediated neuronal differentiation. J Neurosci 33:8172-8184.

Weston NM, Sun D (2018) The potential of stem cells in treatment of traumatic brain injury. Curr Neurol Neurosci Rep 18:1.

Willing AE, Das M, Howell M, Mohapatra SS, Mohapatra S (2020) Potential of mesenchymal stem cells alone, or in combination, to treat traumatic brain injury. CNS Neurosci Ther 26:616-627.

Xiong LL, Hu Y, Zhang P, Zhang Z, Li LH, Gao GD, Zhou XF, Wang TH (2018) Neural stem cell transplantation promotes functional recovery from traumatic brain injury via brain derived neurotrophic factor-mediated neuroplasticity. Mol Neurobiol 55:2696-2711.

Yasuhara T, Kawauchi S, Kin K, Morimoto J, Kameda M, Sasaki T, Bonsack B, Kingsbury C, Tajiri N, Borlongan CV, Date I (2020) Cell therapy for central nervous system disorders: current obstacles to progress. CNS Neurosci Ther 26:595-602.

Yuan F, Xu ZM, Lu LY, Nie H, Ding J, Ying WH, Tian HL (2016) SIRT2 inhibition exacerbates neuroinflammation and blood-brain barrier disruption in experimental traumatic brain injury by enhancing NF-κB p65 acetylation and activation. J Neurochem 136:581-593.